Searching for Lorentz Invariance Violation at the LHCb

Bachelor's Thesis in Physics

Author:
I. L. Dijck

Supervisors:
Dr. H. W. Wilschut
Dr. C. J. G. Onderwater

Abstract

Recent work at the Van Swinderen Institute on Lorentz invariance violation (LIV) in weak interactions, has led to a formulation that suggests possible experimental searches for LIV in weak decay. All laws of physics are supposed to be invariant under the Lorentz transformations from special relativity. This means they do not depend on velocity boosts and rotations of inertial frames. Many modern theories that go beyond current physics question this absolute symmetry. Lorentz violation is expected to modulate decay rates in certain directions, relative to some absolute frame of reference. Theory shows that if such decays occur with high energies (Lorentz factors $\gamma > 100$) spectacularly increased sensitivity to LIV can be obtained. The experimental setup used cannot be rotated and therefore has to rely solely on Earth's rotation when searching for LIV effects. The data used for the analysis comes from the LHCb experiment at CERN, with moderate γ factors.

Van Swinderen Institute for particles physics and gravity
Rijksuniversiteit Groningen

June 2015

Contents

Introduction

Lorentz invariance means that no inertial frame is preferred over another. In more practical terms it says that the laws of nature are covariant under changing orientation or boost velocity. In light of general relativity this seems perfectly natural, but now many theoretical models have been put forward, especially those combining quantum theory and gravity, that violate Lorentz invariance. Thus searching for Lorentz Invariance Violation puts limits on those theories and models. LIV is connected with CPT violation, a fundamental symmetry in quantum theory. Violating CPT symmetry means that Lorentz symmetry must also be violated, but not neccesarily vice versa.

Work at the Van Swinderen Institute on Lorentz invariance violation (LIV) in weak interactions has led to a formulation that suggests possible experimental searches for LIV in weak decays. Theory shows that if such decays occur with large boosts (Lorentz factors $\gamma > 100$) spectacularly increased sensitivity to LIV can be obtained.

The Large Hardron Collider (LHC) is currently by far the largest and most powerful particle accerlator in the world. Its aim is to allow physicists to test the predictions of different theories of particle physics. The main drive was to prove the existance of the Higgs boson, but it's also quite capable of testing other theories. LHC contains seven detectors: ATLAS, CMS, LHCb, ALICE, TOTEM, LHCf, MoEDAL. Each designed for certain kinds of research, The data used in this thesis comes from the LHCb experiment. Proton-proton collisions are the main mode of operation for the LHC. Not only is it the largest particle accelerator, it also uses the largest computing network. This is needed for processing the immense amounts of data that comes out of the LHC experiments. To keep data streams manageable most of the data is thrown away instantly while selections are made about what is usefull to keep and what isn't.

This thesis is mainly about looking for a LIV signal by analyzing the data from the LHCb experiment. The data available for this thesis was collected in 2011 and 2012. There is a difference between the years in terms of both energy and number of events observed. The LHC has restarted on June 3 2015 after a planned upgrade in 2013 and 2014. It is currently performing at roughly 13 *TeV* total beam energy, almost twice that of 2012. All analysis of the data has been done in the ROOT CERN data analysis framework, using scripts in C++. This framework has been made specifically to handle the large amounts of data from LHC experiments.

It will be shown that no significant LIV signal has been found in the specific data set considered in this thesis, consistent with previous limits found for Lorentz Invariance Violation at $\gamma \approx 1$.

Ivar Dijck – `I.L.Dijck@student.rug.nl`

Chapter 1

Lorentz Invariance Violation

In this first chapter, some background information about LIV is given.

Lorentz tranformations are used to go from one inertial frame of reference to another. Invariance means that no inertial frame is preferred over another. As an example; particles going in one direction can not experience a higher average decay rate than particles going in the opposite direction, relative to some frame of reference. If they do, this is called Lorentz invariance violation (LIV). A difference in decay rate for one direction to another is what we will be looking for. Any LIV will neccesarily be a very small effect since all experiments to date have not found any evidence for it ref.[4].

1.1 Lorentz Transformations

The most simple form of the Lorentz tranformations is going from one cartesian coordinates system to another identical one, apart from a boost in x. These coordinate systems are also called inertial frames of reference. The Lorentz transformations on spacetime coordinates, can be represented in matrix form as below ref.[8].

$$\begin{pmatrix} t' \\ x' \\ y' \\ z' \end{pmatrix} = \begin{pmatrix} \gamma & -\gamma\beta & 0 & 0 \\ -\gamma\beta & \gamma & 0 & 0 \\ 0 & 0 & 1 & 0 \\ 0 & 0 & 0 & 1 \end{pmatrix} \begin{pmatrix} t \\ x \\ y \\ z \end{pmatrix}$$

A simple form of LIV would be if there are small additional factors in this matrix. For the specific LIV study here this is not the case. Instead using the standard model extension framework.

1.2 Standard Model Extension

To better study CPT symmetry and Lorentz invariance violation a new theoretical framework was needed. One that combines both the standard model aswell as any CPT/Lorentz symmetry breaking terms. This became an effective-field theory for studying the breaking of these symmetries, now known as the standard model extension (SME). The terms that go into this model have certain leading coefficients. These coefficients can lead to Lorentz symmetry breaking. An example would be for a certain kind of particle to have a slightly higher rate of decay in a certain preferred direction, which depends on the LIV and the leading coefficients in the SME.We won't go into more details of this, but it is used in the literature to define the different parameters involved in Lorentz symmetry breaking ref.[4].

1.3 Gamma Factor

The gamma factor, or Lorentz factor is in layman's terms a measure for how far you are into the relativity regime, as opposed to the classical regime. The Lorentz factor is defined as the factor by which time dilation, length contraction and mass increases when an object is viewed from a moving frame compared to the object's rest frame. To calculate the Lorentz factor we used eq.1.1.

Time dilation means that the mean lifetime of a particle in a boosted frame will be longer than when measured at rest. Thus we would like to compare lifetimes in frames of reference with the same boost velocity. The LIV effect we are looking for shows a pronounced γ dependance. Compared to the standard model the LIV effect on mean lifetime is proportional to γ^2 ref.[8].

$$\gamma = \frac{1}{\sqrt{1-\beta^2}} = E/m_0 = \sqrt{p^2 + m_0^2}/m_0 \tag{1.1}$$

1.4 Sun Centered Frame

Since LIV is dependent on the frame of reference one cannot directly compare one with the other. For all the experiments on LIV to be comparable they have to be in the same frame of reference. A usefull inertial frame of reference to use is the sun centered celestial equatorial frame. In this frame the origin is the Sun, with the Z-axis pointing along Earth's rotation. This frame can be considered fixed in boost velocity and orientation for our purposes, which is needed since any LIV terms may vary with both coordinates.

Anything pointing exactly along the Z-axis would not show any variation of the LIV factor with sidereal time (see chap.3). The LHCb detector is not orientated along the Z-axis, but neither is it perpendicular to it. Instead it makes a $\phi_0 = 52^\circ$ with the Z-axis, see ref.[5] for the full derivation. This means that we can expect a sidereal variation of the LIV factor, which will be what we are searching for.

Chapter 2

The LHCb Experiment

In this chapter, some background information about the LHCb experiment is given.

2.1 The LHCb Experiment

The experiment was mainly designed to study B-mesons, a frequent product of proton-proton collisions. This is also where the name of the experiment came from. Bottom quarks, i.e. b-quarks, were known as beauty quarks shortly after discovery, thus the LHC beauty experiment, LHCb.

Proton-proton collisions is the main operating mode for the LHC. Lead nuclei can also be used for collisions, usually about 1 month per year is reserved for this. The particles that are to be used in the the main LHC ring first need to be created in a source and accelerated before entering. Protons go in order through the LINAC2, PSB (Proton Synchrotron Booster), SP (Proton Synchrotron), SPS (Super Proton Synchrotron) in this order, before finally entering the LHC main ring at around 450 GeV. Here they are accelerated to their final energy ref.[2].

2.2 The LHCb Detector

The LHCb detector is an asymmetric setup. This means that only the forward scattered particles can be detected. The physical length is about 20 m, a large detector is needed or the decay products might escape before being observed.

The detector is made up out of several detector components, all specializing in different measurements. The main purpose is to track and identify the many particles being produced. In order of distance we have: ref.[2]

- Vertex Locator (VELO): A large number of Silicium strip-detectors, only millimeters removed from the beam.
- RICH1: Ring Imaging Cherenkov radiation locator. Cherenkov radiation comes from charged particles moving through that medium faster than light.
- TT: Another set of different Silicium detectors for tracking the particles.
- Magnet: The path of charged particles is bend in a magnetic field, helping to easily seperate charged from non charged particles, aswell as the sign of the charge. Furthermore can accuratly determine the momentum of such charged particles.

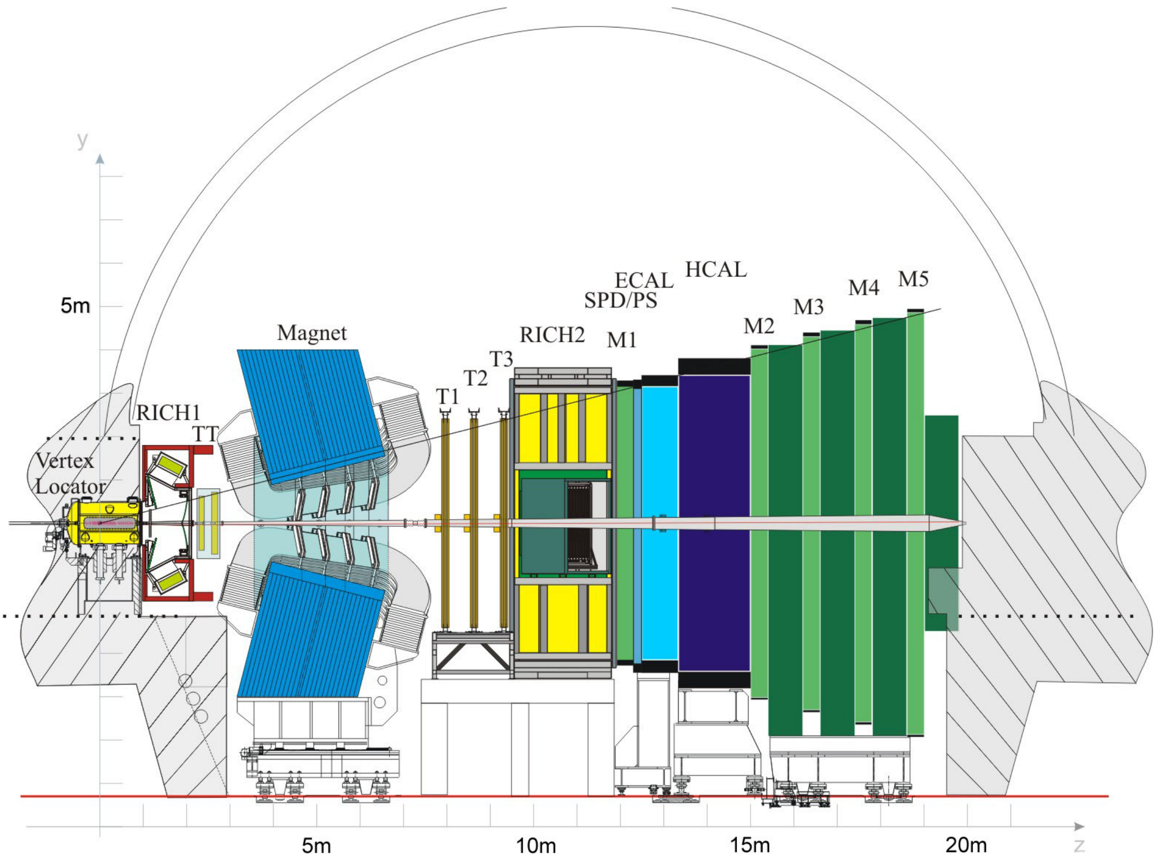

Figure 2.1: Shows the schematic for the LHCb detector.

- T1-3: A set of gas tubes that ionizes if high energy particles move through. Provides a similar role as the TT detectors.
- RICH2: A second detector of Cherenkov radiation.
- M1: A detector specializing in the indentification of muons.
- ECAL: Electromagnetic calorimeter for measuring the energy of electrons and photons.
- HCAL: Hadronic calorimeter for measuring the energy of neutral hadrons mainly.
- M2-5: The rest of the muon detectors.

2.3 Track Types

There are two main track types used in this analysis, long track and downstream track. Track types in the detector is a way to identify the kind of path the particle has followed. The main difference between these two is where the particle has decayed. For the downstream track it is after the first set of velo detectors instead of before, while both go through both sets of trackers (TT and T1-3) see fig.2.2. The most important thing to be said about them is that the gamma distribution for both tracks are fairly similar. This is why we decided to simply add both of them together in the analysis instead of treating them apart. However there is a very clear difference in average decay pathlength between them (as could be expected). Moreover the downstream track has many times more data total ref.[1].

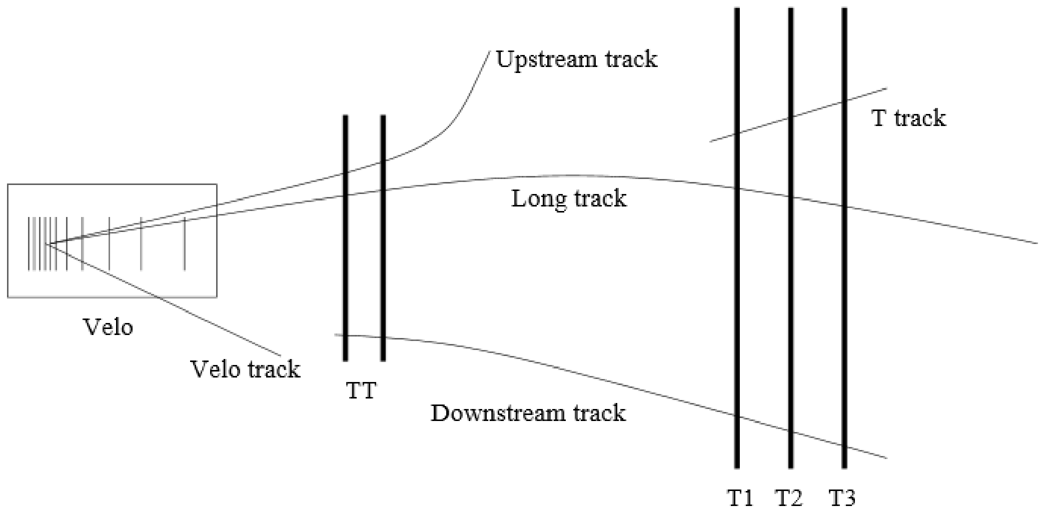

Figure 2.2: Shows the different kinds of tracks there are. Of main concern are the long and downstream tracks.

2.4 Reconstruction

The LHCb incorporates the data from all of the different detector components to reconstruct the path the particle actually took, aswell as the properties it has. The raw data consists of a set of vertices were the particles has been measured. Most of this low level analysis is done immidiatly after the measurements, and everything that isn't found to be sufficiently "interesting" is discarded. To correctly identify particles these events have many parameters indicating different certainties in relation to this reconstruction. Apart from selecting data with some of these parameters, we did not redo any of these reconstructions. Our analysis makes use of the outcome of this low-level analysis.For example, the track-fitting quality and particle identification were used in our analysis. We tighten these conditions considerably (see chap.4). In this way background events are eliminated, but at the same time we lose some of our signal events thus these conditions cannot be too strict.

2.5 Lambda Particle

The lambda particles (Λ^0) studied in this thesis are made up of 3 quarks: up, down and strange. The most common decay mode for the particle (Λ) and anti-particle ($\bar{\Lambda}$) are mediated by the weak force and are given by eq.2.1 and eq.2.2 respectively. The rest mass of the Λ is $m_0 = 1115.683 \pm 0.006$ MeV. The mean lifetime of the Λ is τ_0=2.631 $\pm$ 0.020 $\cdot$ 10^{-10} s ref.[3].

$$\Lambda \rightarrow p + \pi^- \tag{2.1}$$

$$\bar{\Lambda} \rightarrow \bar{p} + \pi^+ \tag{2.2}$$

Chapter 3

Methodology

This chapter is about the general method used in the analysis.

The decay rate of the Λ is related to the mean lifetime. Longer mean lifetime, lower mean decay rate. Lower mean decay rate, longer mean decay pathlength. Decay pathlength is the variable we consider in our analysis.

3.1 Sidereal Time

To test potential preferred frames of reference we would like to be able to turn the setup in another direction. Of course the LHC itself can't be turned. However it does turn together with the orientation of Earth, and will point in a different direction in the sun centered frame of reference after some time. The variable that matters is then the relative direction that the detector points at, at that time. This direction can be expressed in sidereal time, in 24 hour periods instead of 360 degrees. A full rotation in absolute space takes exactly one sidereal day. This is slightly less than a "normal" Earth day. The GPS timestamp in the datafile can be converted to sidereal time indicating a direction [7].

If there is a LIV signal it will show up as a small sidereal variation in a particular observable. However there may be systematic shifts causing apparent sidereal variations. When combining all data over a year for a single sidereal period (3 sidereal hours) you would expect most of these systematic effects to average out.

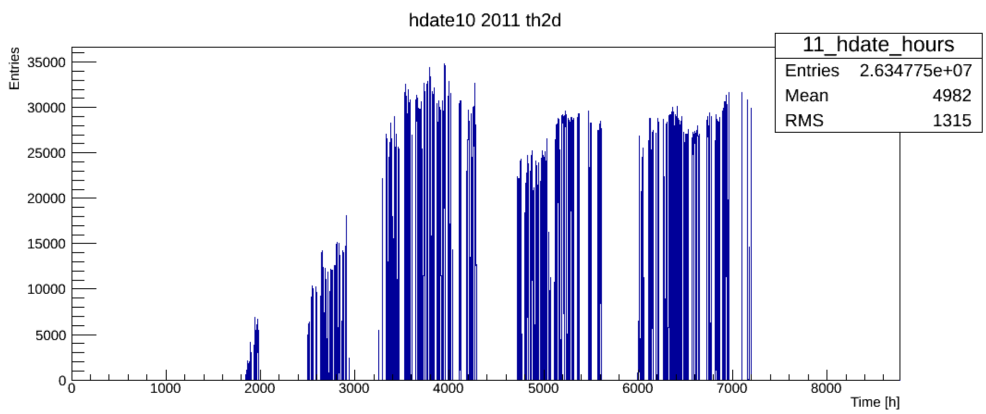

Figure 3.1: The data collected in the year 2011. Most data was collected during the summer months. Sidereal time was defined as 0 h at 1-1-2011 00:00

3.2 Comparisons

At first we wanted to compare an observable for a sidereal time with the same sidereal time half a year later. Thus dividing out any effects from the detector. This turned out not to work well because the data is largely set in the summer and not evenly distributed (see fig.3.1 and fig.3.2). The data is strongely fragmented roughly in patches of 8 hours data and 8 hours rest.

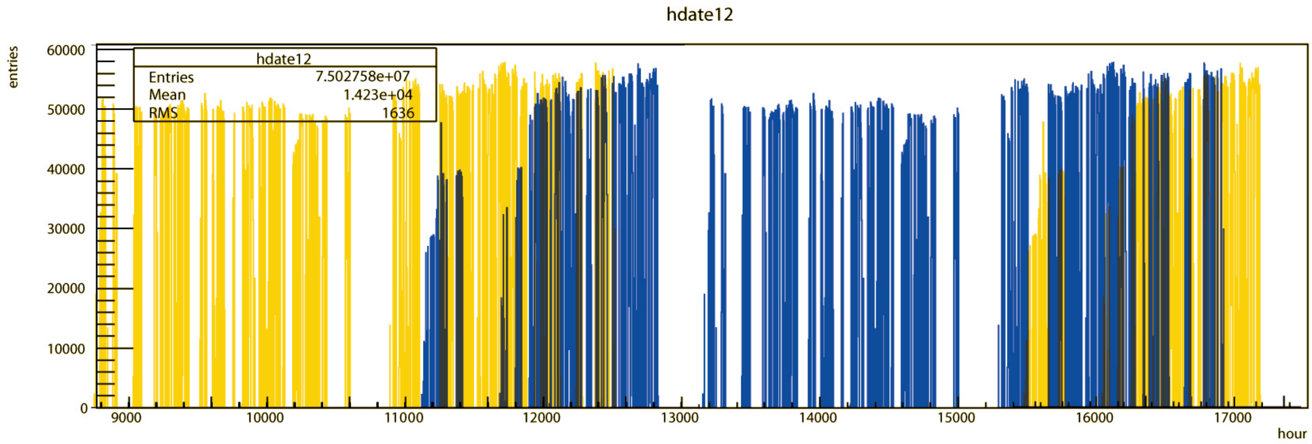

Figure 3.2: Shows when the data was collected in the year 2012 and the overlap with half a year offset. Blue shows when the data was collected. Yellow is the same data distribution shifted by half a year, modulo one year, to show the overlap.

The total energy was increased from 7 TeV to 8 TeV between the 2011 and 2012 dataset, and the average events per hour was more than doubled. Small changes could also be seen in either the trigger or the software going from 2011 to 2012.

Because of the data scatter we choose to compare an observable for a single sidereal period over the whole year with the same sidereal period 12 h later. This would also get rid of systematic shifts while keeping the sidereal variation from LIV. This does not get rid of all detector acceptance components however. By analysing the data in bins of gamma we could more easily recognize a LIV signal. Helping to suppress systematic errors which may also exhibit a gamma dependance, see sec.3.4.

3.3 CERN ROOT

All analysis of the data has been done in the ROOT CERN data analysis framework, using scripts in C++. This framework has been made specifically to handle the large amounts of data from LHC experiments. ROOT is a framework in C++ to add extra functionallity to C++ as a language. ROOT is made to do some memory management, aswell as give you easy acces to make histograms. It is a widely used program in the particle physics community. The datafiles from the LCHb experiment used in this thesis are more than 130 GB in total size and it took roughly half an hour to fully analyse the 10^8 events on the used computer [6].

3.4 Gamma Bins

To better know if we truely found a LIV signal and not just a statistical fluke we separated the data into 3 different gamma bins. We would expect to find a larger LIV effect at the higher gamma bin since the LIV part of the decay rate is predicted to go with a factor γ^2. In fig.3.3 the γ (boost) distribution is shown and the three seperate γ bins for our analysis are indicated.

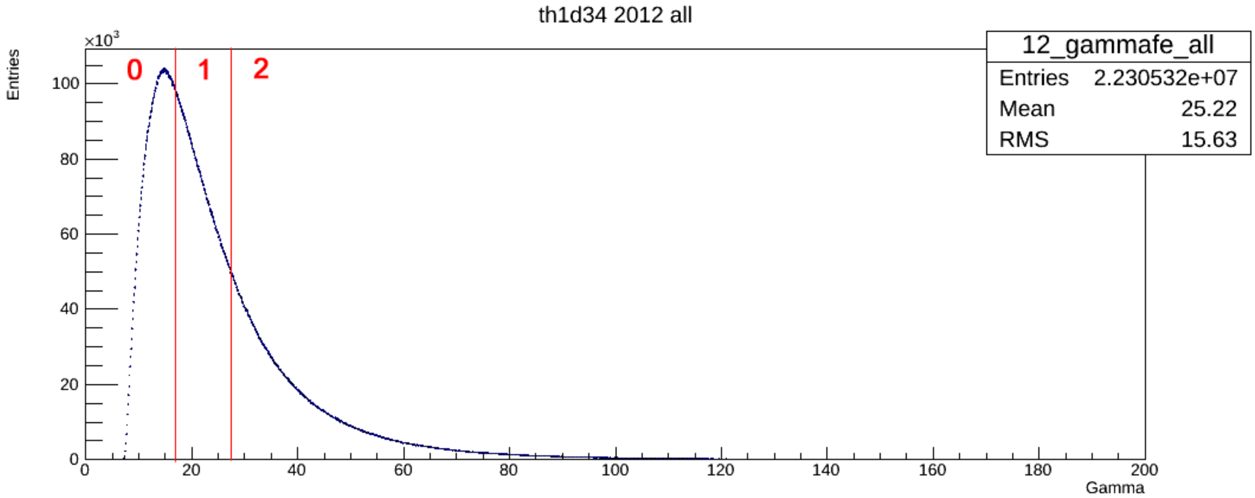

Figure 3.3: The γ distribution for the 2012 selection. Included are the bin sizes used at roughly the same area each. gamma's used in bin 0,1,2 are from 0 to 16 to 27 to 200 respectively.

Chapter 4

Data Selection

The data acquired from the LHCb experiment has already been analysed to some extent. The raw detector output has been converted to usefull Λ canditates properties like decay pathlength and invariant mass. Nevertheless the data file itself does not only contain the Λ particles we are looking for. There is still background consisting of Λ candidates by very loose standards of the primary data selection. To get a higher signal to background ratio we used several selection criteria to improve the Λ selection.

4.1 Lambda Mass

The main observable we considered for the selection is the reconstructed invariant mass. Invariant mass is a value that is always the same in any frame of reference, thus invariant. It is calculated from the momenta of the decay products. All reconstructed particles we want must have an invariant mass close to m_0. Furthermore Λ particle candidates are required to decay into one proton and one pi meson. These particles are both charged, unlike the Λ itself ref.[3].

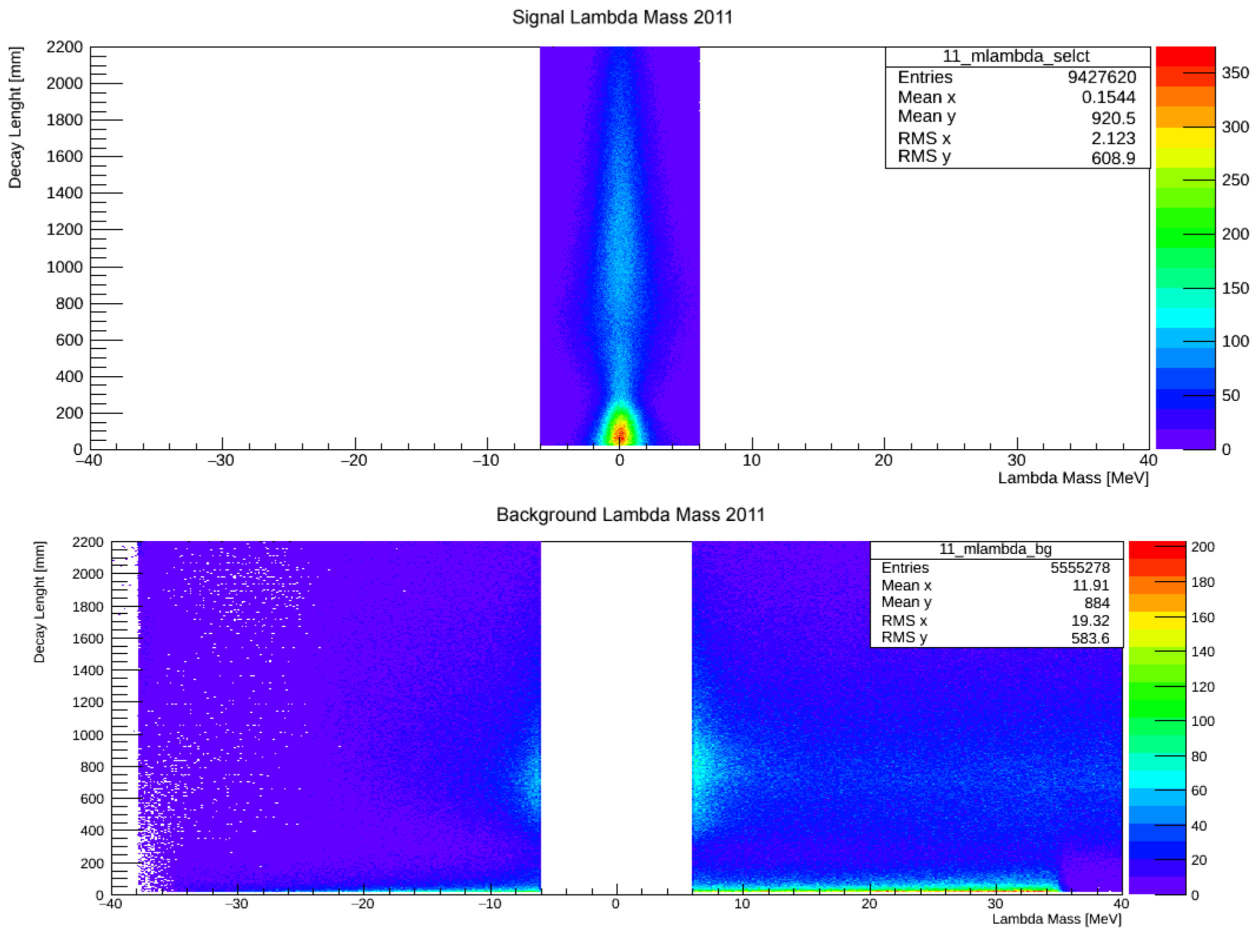

Figure 4.1: Shows the range of masses for the events around the rest mass for a Λ particles in the signal (top panel) and background (bottom panel) area.

There are several branches in the data with information about the probabilities for particles actually being correctly identified. We define our signal area as everything between -6 MeV $< |m - m_0| <$ 6 MeV and the background area as the rest as shown in fig.4.1.

For these two areas we will now look at some of the selection criteria to get rid of even more background noise from the signal area. With this setup we can look at the distribution for the signal and the background areas to look for significant differences, and put in selections for the signal area.

4.2 Selection criteria

For the neural network probabilities such a difference was found for pi (see fig.4.2), but not as strong for the proton. Most likely because a significant amount of the background consists of protons already, but not pi's. Setting the probability for the pi to be atleast 0.1 gets rid of some of the background while retaining most of the signal.

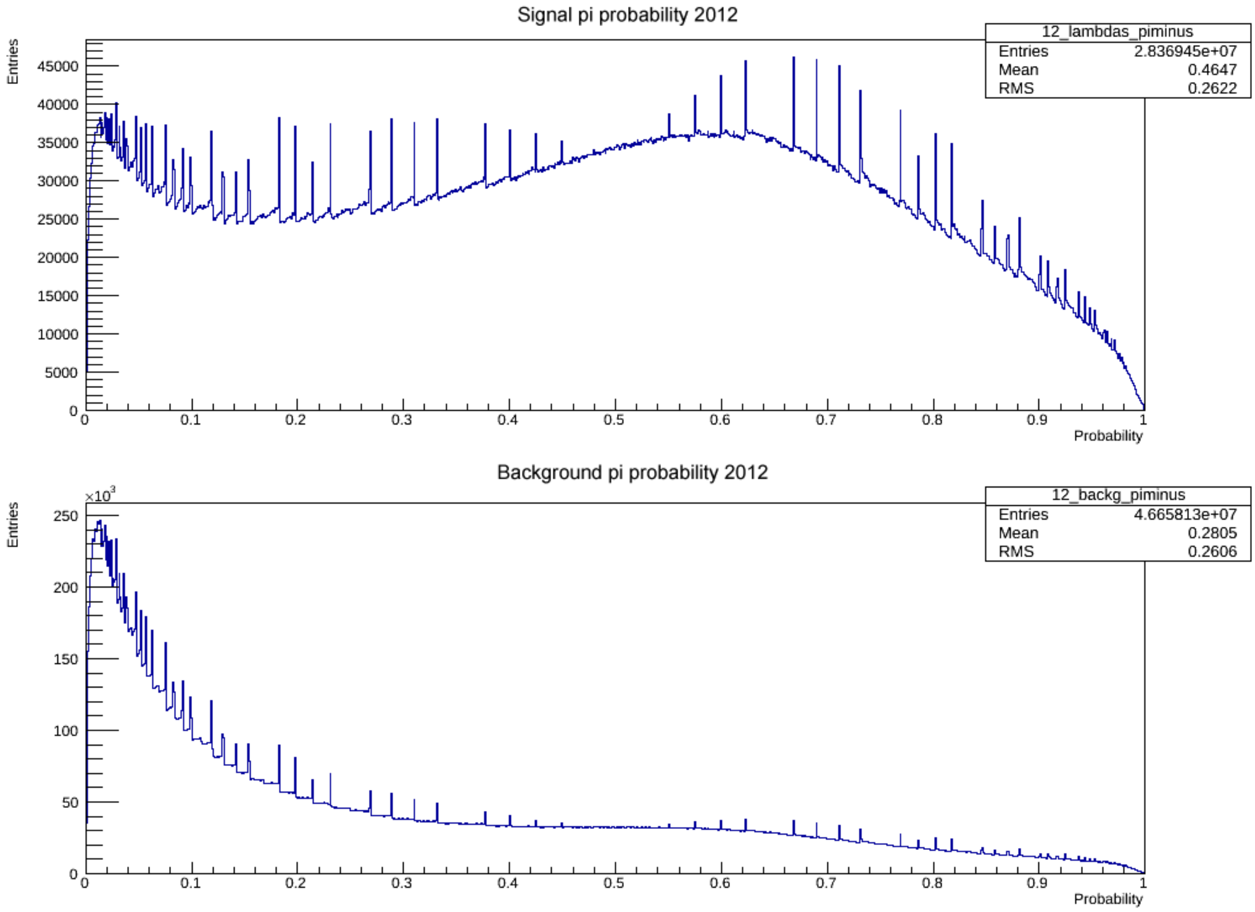

Figure 4.2: The distribution of probabilities determined by a neural network for the pions to be a real pion particle, in the signal (top panel) and background (bottom) area of invariant mass.

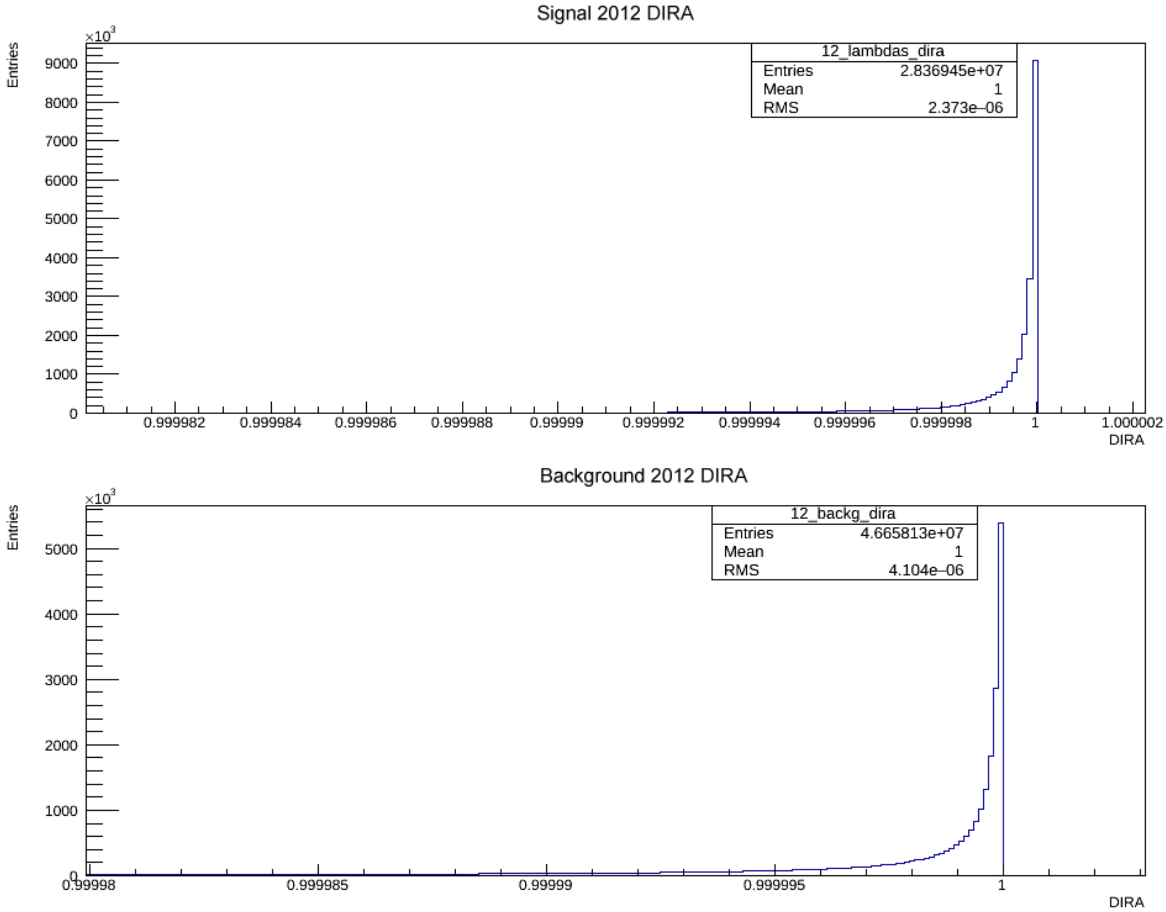

Figure 4.3: DIRA distribution in the signal (top panel) and background (bottom) area of invariant mass.

Similar ways are used to require DIRA > 0.99999 (see fig.4.3) and FD $\chi^2 > 5$ (see fig.4.4). DIRA (diraction angle) evaluates the cosine of the angle between the reconstructed momentum of the particle and the vector connecting the primary vertex with the decay vertex. FD χ^2 (flight distance) is related to the strenght of the fit from the primary to the secondary vertex. The exact definitions are not actually important to us as long as there is a clear difference between the background and signal areas from fig.4.1 ref.[1].

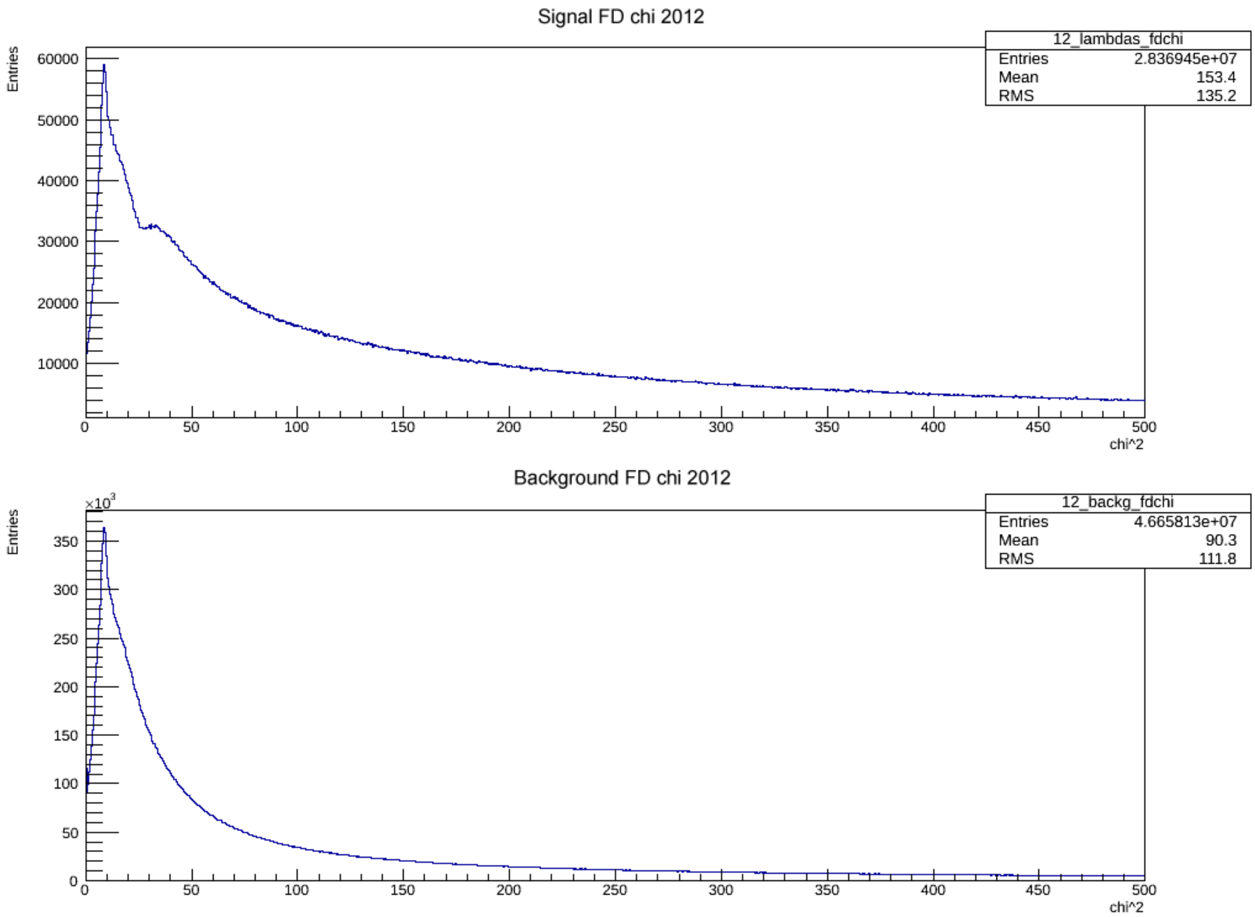

Figure 4.4: FD χ^2 distribution in the signal (top panel) and background (bottom) area of invariant mass.

The lower bound of 20 mm for the decay pathlength came from looking at 4.1, it shows that decay pathlength shorter than 20 mm most likely are not real Λ's. The upper bound of 2200 mm came from the same picture that showed a bump around 2500 mm. Looking at the schematic in fig.2.1 this bump may be caused by the detector.

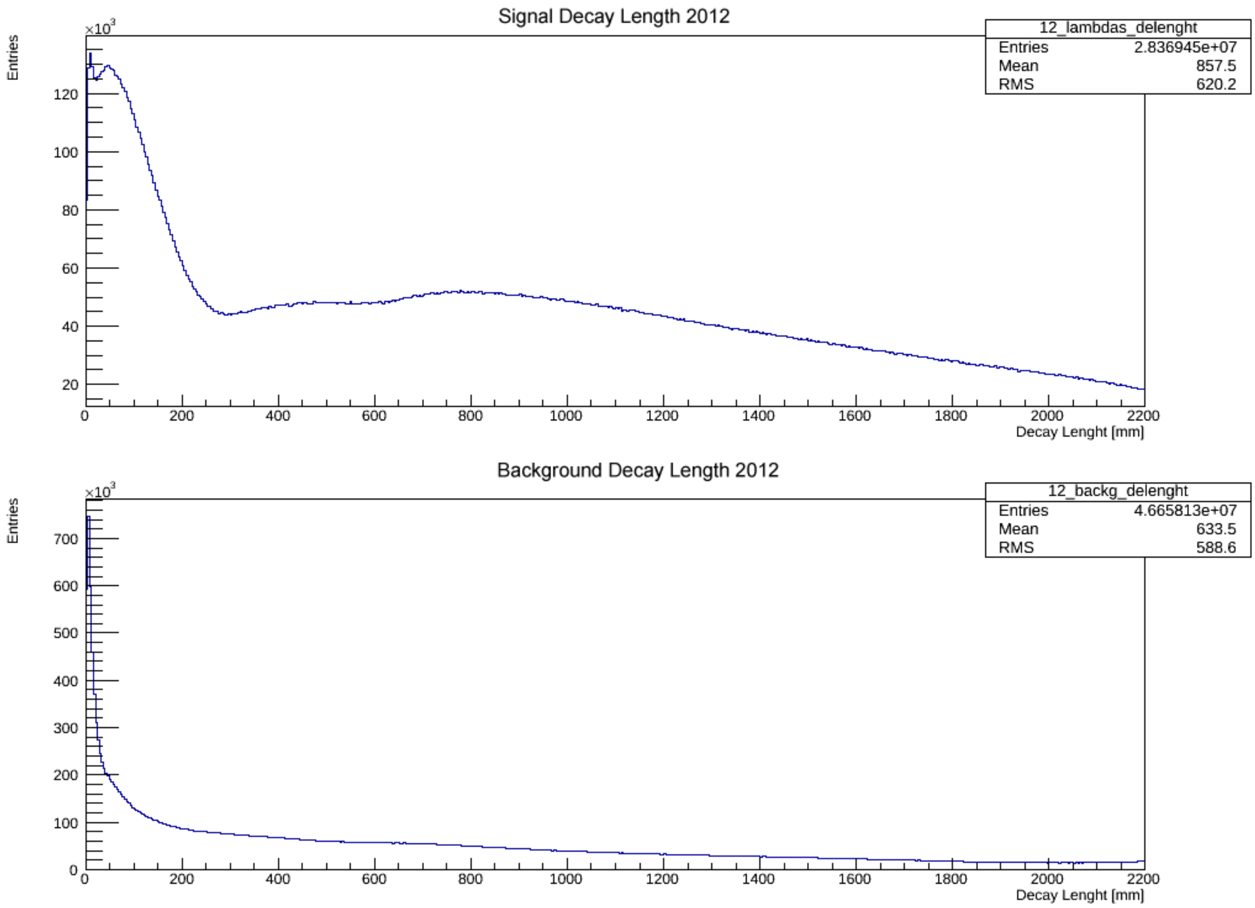

Figure 4.5: Decay pathlength distribution in the signal (top panel) and background (bottom) area of invariant mass.

4.3 Sidereal Selection Effect

The selections discussed in the previous section left us with roughly one third of the Λ candidate events for both years (0.36 and 0.30 for 2011 and 2012 respectively). Since we are looking for sidereal variations we checked wether the selections we made had introduced a sidereal variation. A small effect was found (fig.4.6), so we have to make sure that it can be removed by taking the appropriate asymmetry ratio.

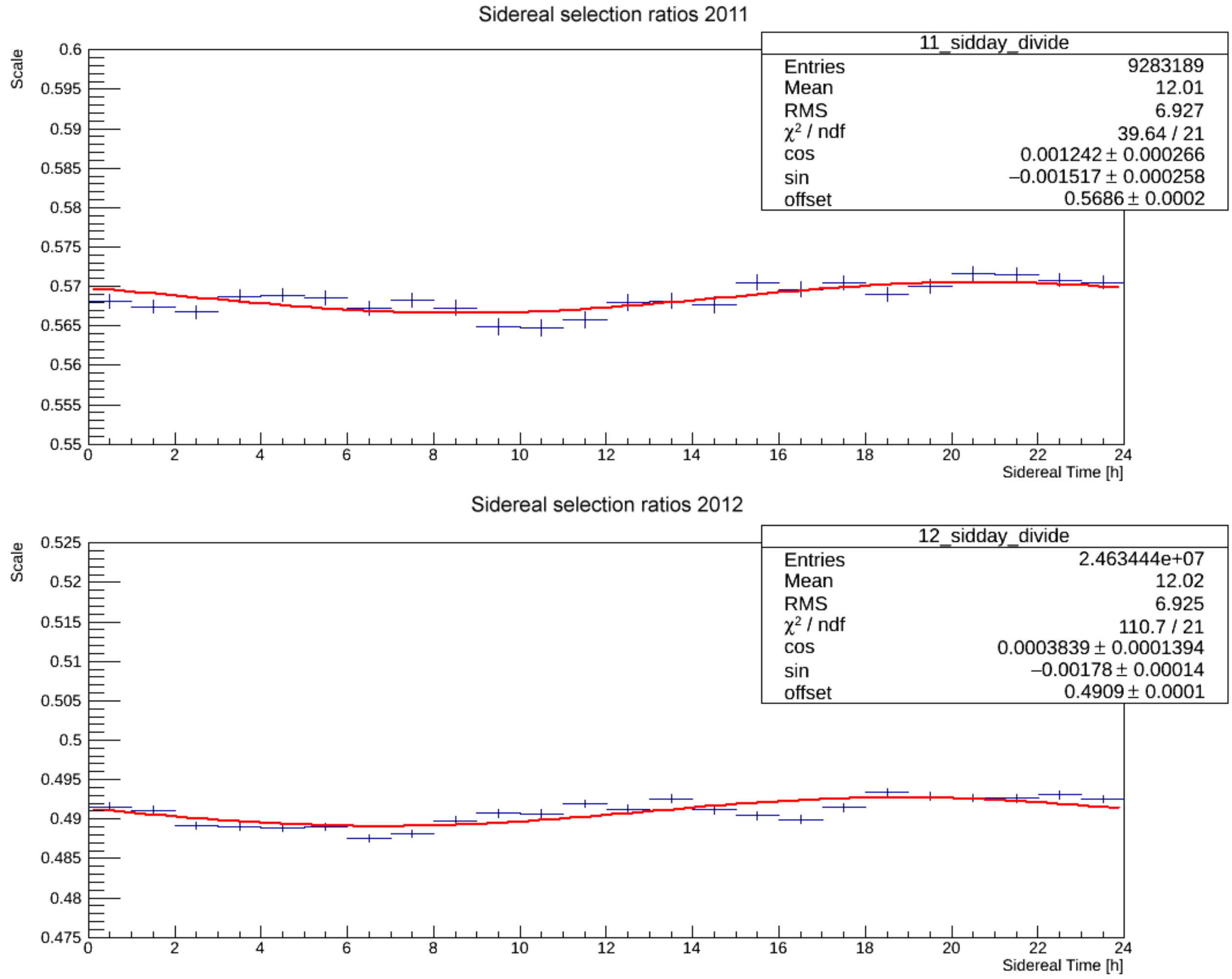

Figure 4.6: Shows the small sidereal effect introduced by the selection criteria. The x-axis is the number of signal events divided by the number of background events.

Chapter 5

Analysis

One of the main problems is that one time period may have a much higher production of events than another. Furthermore not only the production but also the detector acceptance may have changed in between time periods. Certainly from 2011 to 2012, which is one of the reasons they are analysed seperately. To remove these effects we take the asymmetry ratio

$$A^i(L) = \frac{R^i(L) - \alpha B^i(L)}{R^i(L) + \alpha B^i(L)} \tag{5.1}$$

Here R (fig.5.1) and B (fig.5.2) are decay pathlength histograms for a 3h time period, and the time period plus twelve sidereal hours respectively. By the normalization α (eq.5.2) we set the average offset of $A(L)$ to zero. The four different time periods of 3h all have their own R's, B's, A's and α's.

$$\alpha = \frac{\int_{0mm}^{2200mm} R(L)dL}{\int_{0mm}^{2200mm} B(L)dL} \tag{5.2}$$

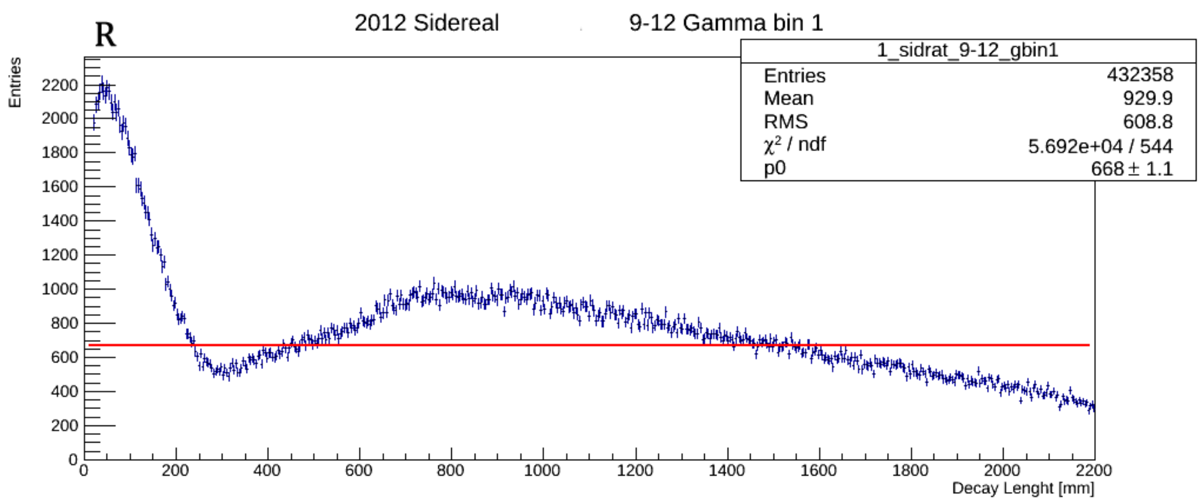

Figure 5.1: The decay pathlength spectrum for $\bar{\Lambda}$'s in 2012 in gamma bin 1, sidereal time from 9 to 12. The mean fit (p0) is used for determining α, equal to the average integral of the counts.

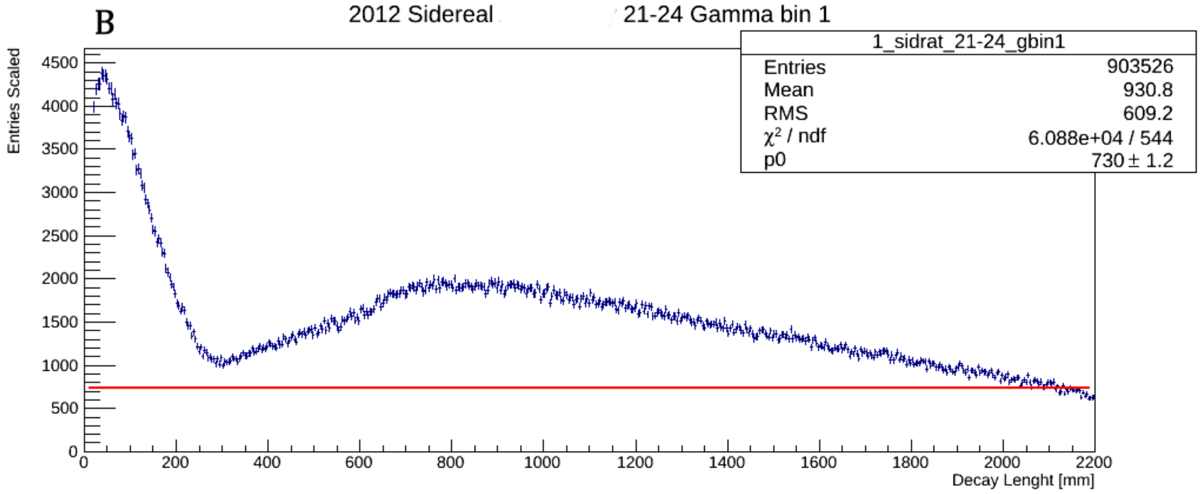

Figure 5.2: As in fig.5.1 but for sidereal time from 21 to 24, 12 hours later than fig.5.1. The mean fit (p0) was used to determine α, before being divided by α.

The proper error margins per bin are dependent on both R and B since the numerator and denominator in the asymmetry relation (eq.5.1) are not independent either.

$$\sigma_{A(L)}^{i}{}^{2} = \frac{4\alpha^2 (R^{i2}(L)\sigma_B^i{}^2 + B^{i2}(L)\sigma_R^i{}^2)}{(R^i(L) + \alpha B^i(L))^4} \tag{5.3}$$

σ_R^i and σ_B^i are the errors in $R^i(L)$ and $B^i(L)$ from fig.5.1 and fig.5.2. We did not take into account the error in α since it is very small compared to the errors in $R^i(L)$ and $B^i(L)$.

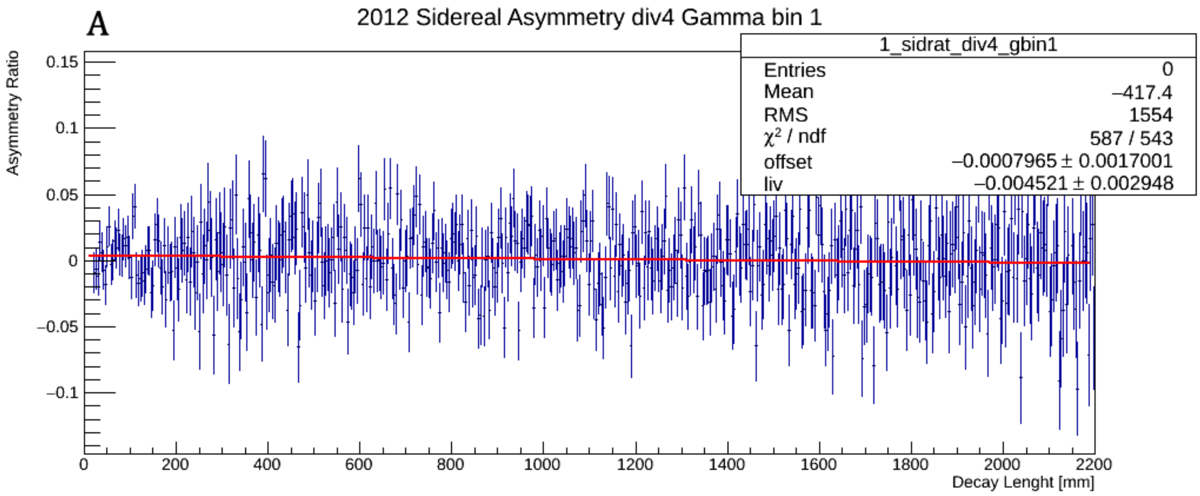

Figure 5.3: Variations of just one of the asymmetry ratio for the decay pathlength range. Made from the anti particles in 2012 in gamma bin 1, sidereal time period 4. The given parameters of the fitted function offset and liv are A_o and $\alpha_{LIV}\langle\gamma^2\rangle$ respectively.

$A(L)$ is fitted with the function $f_A(L)$. Because the asymmetry ratio depends in a complicated way on the distribution of observed gammas, there is no simple way to derive an analytical expression for the asymmetry. But a usefull approximation is given by the function

$$f_A(L) = (1 - 2 \cdot A_o^2)\alpha_{LIV}\langle\gamma^2\rangle(\frac{L}{L_0 \cdot \langle\gamma\rangle} - 1) + A_o \tag{5.4}$$

The two free parameters were fitted to the asymmetry ratio's as seen in fig.5.3. These parameters are A_0 and a parameter containing the LIV, $\alpha_{LIV}\langle\gamma^2\rangle$, which is our signal. The two remaining parameters are, $L_0 = \tau_0 c = 78.88$ mm and $\langle\gamma\rangle$ is given by

$$\langle\gamma\rangle = \frac{\int_0^{200} \gamma N(\gamma) d\gamma}{\int_0^{200} N(\gamma) d\gamma} \tag{5.5}$$

The four values of $\alpha_{LIV}\langle\gamma^2\rangle$ thus obtained can now be used to extract the possible sidereal variation by fitting

$$f_S(h) = A_S \cdot \sin(\frac{2\pi}{24}t) + A_C \cdot \cos(\frac{2\pi}{24}t) + O_\alpha \tag{5.6}$$

as expected from theory. This is plotted in fig.5.4. The three free parameters in this fit function are A_S for the sin coefficient, A_C for the cos coefficient and O_α for the offset parameter. In these plots, O_α has no real physical meaning, sin/cos coefficients are the components of the LIV effect as will be discussed in chap.6.

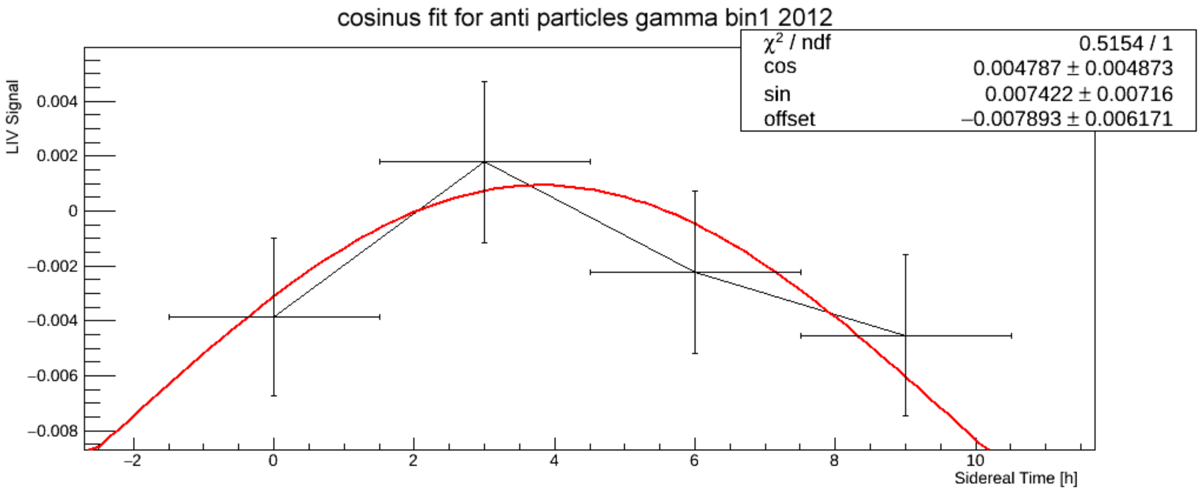

Figure 5.4: The values of the LIV signal $\alpha_{LIV}\langle\gamma^2\rangle$ for the four different sidereal time periods. The sin, cos and offset parameters listed are A_S, A_C and O_α respectively.

Chapter 6

Results

The results from the analysis discussed in chap.5. The 3 different gamma bins are shown in (fig.6.1). Red, green, blue refer to gamma bin 0, 1, 2 respectively, were $x = A_C$ and $y = A_S$. The contours are one σ or 68% confidence limit within which $\alpha_{LIV}\langle\gamma^2\rangle$ should lie. Any correlation between x and y was not taken into account when determining the error contours. The weighted average of the gamma bins is shown in black in fig.6.1. Having two different years and both normal and anti particles gives 4 seperate polar plots in total.

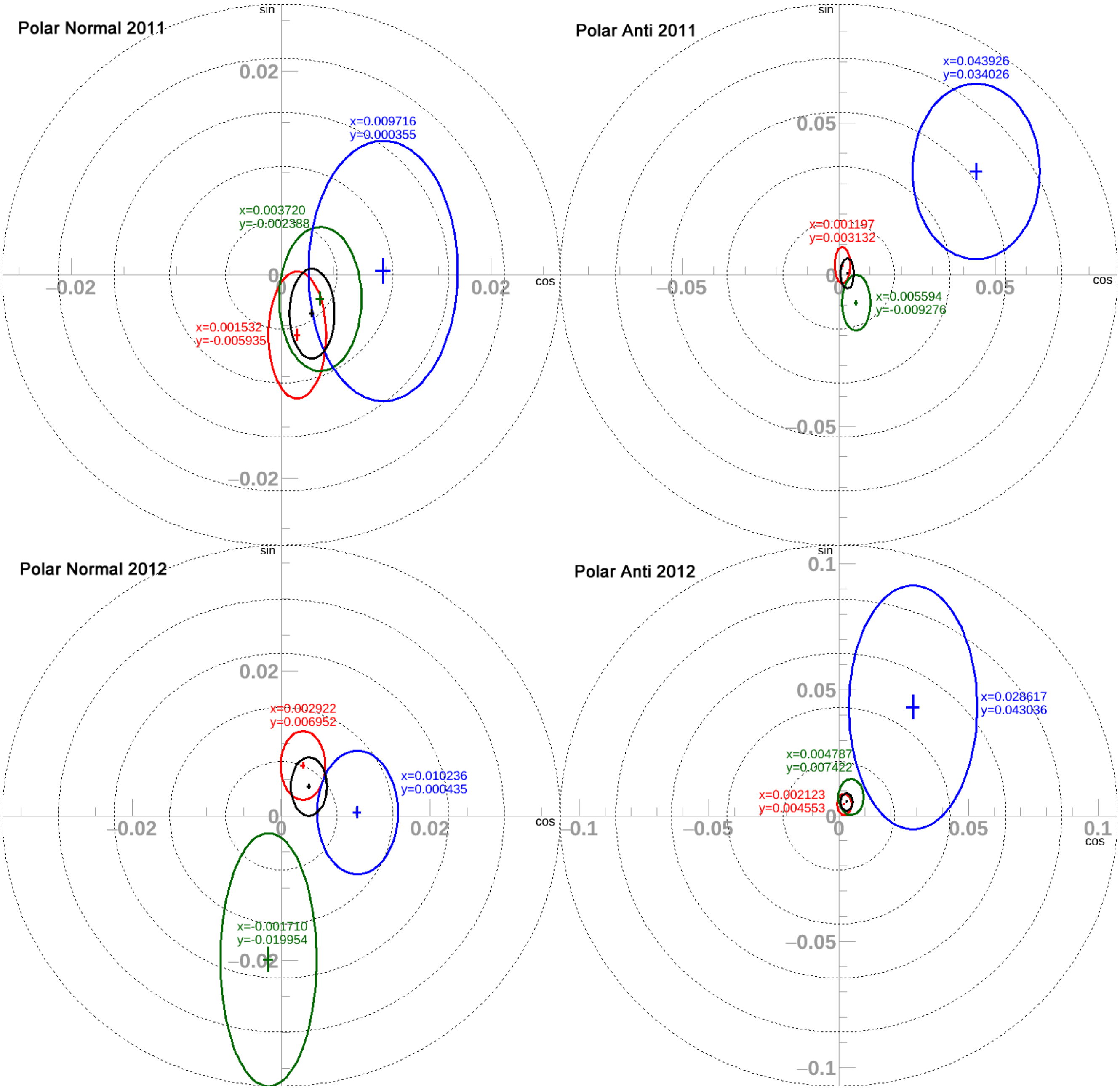

Figure 6.1: The end results plotted in the complex plane for the normal/anti particles in 2011/2012.

6.1 Comboplot

To get the very final result we calculated the wheighted mean of all the polar plots combined into one. Because the LIV effect we analysed is CPT-even we can simply add the anti particles.

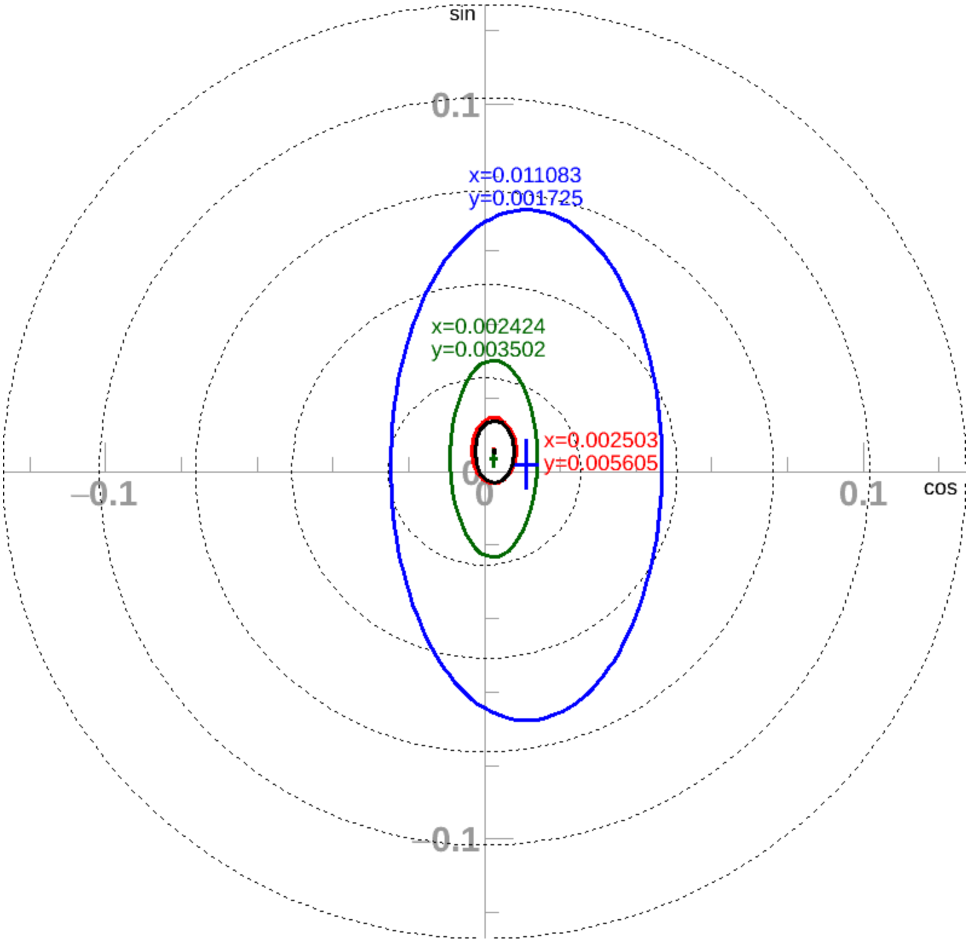

Figure 6.2: The final result of adding all the different polar plots into one.

In this plot $r = \alpha_{LIV}\langle\gamma^2\rangle = \sqrt{x^2+y^2}$ is the size of the LIV effect. With $\langle\gamma^2\rangle = 882.2$, $x = 0.0027$ and $y = 0.0053$ this comes out as $\alpha_{LIV} = 9.2 \cdot 10^{-5} \pm 1.5 \cdot 10^{-4}$.

Discussion and Conclusions

In this bachelor's thesis we wanted to know wether we could measure a Lorentz Invariance Violation (LIV) signal. Such a signal would point towards physics beyond the standard model.

To try and get at such a potential LIV effect we used the data from the LHCb experiment. This data contained the decays for lambda (Λ) particles. Λ particles decay mainly via the weak interaction into one proton and one pi meson.

The LIV effect is enhanced by γ^2 with regard to the standard model. Thus particles with a high Lorentz factor would be expected to display a larger LIV effect than the same particles at a lower Lorentz factor.

The analysis cosisted mainly of comparing the entire dataset for one sidereal time period (direction) to another 12 hours later for a certain gamma range. This way most other sidereal effects should average out.

The result found ($\alpha_{LIV} = 9.2 \cdot 10^{-5} \pm 1.5 \cdot 10^{-4}$) is consistent with zero within the error margin. This is the case both for the average of all the gamma bins combined aswell as the gamma bins seperate. Thus if there is a Lorentz symmetry violation it is smaller than what could be found in this research for this specific dataset.

Bibliography

[1] *TWiki at CERN*,NilsHoeimyr (r44 - 2014-01-27)
`https://twiki.cern.ch/.`

[2] *The LHCb Detector*, CERN (2008)
`http://lhcb-public.web.cern.ch/lhcb-public/en/detector/Detector-en.html`

[3] *Particle Data Group*, C. Amsler et al. (2008)
`http://pdg.lbl.gov`

[4] *Lorentz violation in weak decays*, Jacob Noordmans (November 2014)

[5] *Search for CPT and Lorentz violation in B^0 mixing with $B^0 \to J/\psi\ K_S$ at LHCb*, M.C. van Veghel (January 2015)

[6] *ROOT — A Data Analysis Framework - Cern*, The ROOT Team (1995 - 2015)
`https://root.cern.ch/drupal/content/about`

[7] *The new definition of universal time*, Aoki, S. et al. (1982)

[8] *Relativity DeMystified*, David McMahon (2006)

Appendix A

Additional Graphs

All additional graphs used for a full run of the analysis provided externally.